Push-bending Process and Forming Quality of Stainless-steel Tubes

Chen Guo-qing[1,*], *Yang Jian*[1], *Li* Hong-xiang[1], *Fu* Xue-song[1], *Tang* Rui[2], *Zhou* Wen-long[1]
[1]Key Laboratory of Solidification Control and Digital Preparation Technology (Liaoning Province), School of Materials Science and Engineering, Dalian University of Technology, Dalian116085, China
[2]Science and Technology on Reactor Fuel and Materials Laboratory, Nuclear Power Institute of China, Chengdu 610213, China

Abstract. The push-bending process of stainless-steel tubes was investigated by using the experimental method and finite element (FE) analysis based on the commercial software MSC.MARC. The effects of the processing parameters and the lubricating condition on the forming quality of as-obtained ASTM304 tubes were discussed. The results demonstrated that the experiment results were consistent with the simulation both in deformation behaviour and the stress distribution during the push-bending process, which verified the reliability of the established FE-model. The results also show that the maximum residual stress concentrates in the middle of tubes, the residual strain on both the external side increases firstly, then decrease, and increase again with the increase of the location angel. After the push-bending, the interior wall thickness increases while the exterior wall thickness decreases. When the relative bending radius is larger, smaller variation of wall thickness will be obtained. With the increase of the friction coefficient, the wall thickness thinning rate will decrease. With the increase of the pushing speed, the wall thickness thinning rate decrease a little while the thickening rate increases slightly. When push-bending of the large radius tubes, a good lubricating condition can reduce the wall thickening problem at the intrados, which will ensure a better forming quality.
Keyword. Bending, Quality control, Simulation

1 INTRODUCTION

As important lightweight structures and liquid conveying or heat exchanging components, metallic tubular parts are widely used in the fields of aeronautics and aerospace, automobile, oil and chemical industries, etc. It has great advantages of efficiency, cost, and quality when tubular productions are made by plastic forming technologies. Among them, bending is most commonly used [1].

The studies of tube bending mainly focus on the deformation behaviour during the process. The researches on deformation vary from wrinkling instability, cracking, cross section deformation to spring back phenomenon. Yang [2-4] did some works on the wrinkling activity from the effects of parameter to the prediction model. Megharbel [5] introduced a method to analysis bending tubes with different section shapes, and built equations to predict the moment for forming tube to a specific radius of curvature. There are also a lot of studies on spring back. The predicting equation [6-7], the mechanism [8], the time-dependent behaviour [9-10], the effects of different parameters [11] are all included in the study of spring back.

However, most of studies are focus on the rotary bending only. There are few results on the push- bending process. In this paper, a FE model is established to analysis the push-bending process. The model is verified with the experiment from the aspects of the wall thickness and the residual stress. The model is also used to study the contact behaviour during the push-bending. The effects of some parameters on wall thickness are mentioned.

2 Research Method

2.1 Experimental method

The experiments are conducted using hydraulic machine which provides a force of 3150KN, as shown in Fig.1. The mechanism is composed of sleeve, bending die and punch. The stainless tubes of AISI304 are used in the experiment with length l of 250mm. The outer diameter d of the tubes is 34mm, and the thickness t is 4mm. The radius R after the push-bending process is set as 136mm, and the bending angle θ is 90°. During the experiment, engine oil is used as lubricant. The wall thickness of the tube at different locations after bending is detected by ultrasonic generator and oscilloscope. X ray diffraction (XRD) is used to detect the residual stress along extrados of the tube.

2.2 FE method

The finite element model is established using the commercial finite element software MSC.MARC. The element size we used in the simulation is 2mm*2mm. Considering the symmetry character of the tube and the bending process, the model is simplified as a half model. The mechanical properties of the material are shown in

*Corresponding author: gqchen@dlut.edu.cn

Tab.1. The solid shell 182 is used in the model due to the consideration of hourglass and reducing integral function. Coulomb friction law is employed with the friction factor of 0.08. The whole process is divided into two parts, the loading process and the unloading process. During the loading process, the punch is set with a certain velocity.

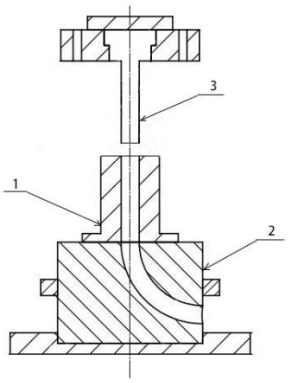

(a)

(b)

Fig. 1. The equipment of push-bending: (a) The Assembly diagram: 1: sleeve; 2: bending die; 3: punch; (b) The real figure.

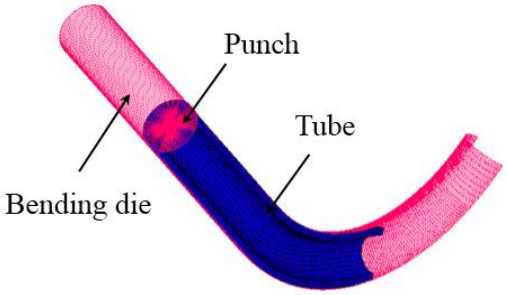

Fig.2. Finite element model of push-bending.

Table 1. Mechanical properties of AISI 304.

Density, ρ(kg/m3)	7930
Young's modulus, .E(GPa)	193
Poisson's ratio, ν	0.3
Tensile strength, σb(MPa)	694.72
Yield strength, σs(MPa)	242.31

2.3 Comparison of the methods

In order to verify the reliability of the finite element model, the results of the experiment and FE simulation are compared in two aspects: the residual stress and the wall thickness.

The results of the wall thickening/thinning of both the experiment and simulation are compared as shown in Fig.3. With the increase of the angle where the points are located, the exterior wall thickness decreases first and then increase. However, the interior wall thickness changes in an opposite rule. The results of both the experiment and the simulation show the same rule. The maximum wall thickness error of experiment and simulation is 3.38% of the exterior wall thickening, and 6.20% of the interior wall thinning.

Fig.4 (a) shows the bent tube in experiment and simulation. The tubes are in good agreement in the shape, and there is no obvious pints on the surface. Fig.4 (b) is the comparative results of the residual stress at extrados. In the loading process, the exterior wall is in the role of tensile stress. When in the unloading process, there will be compressive stress at the extrados. With the increase of the angle where the test points are located, the residual compressive stress increases first and then decrease, and increases again in the location with a larger angle. The gap between simulation results and experiment results may be caused by the residual stress in the original production process and the error of X-ray diffraction method.

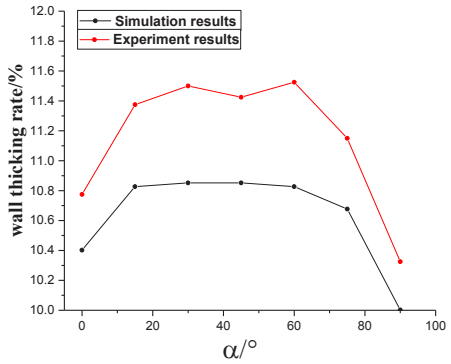

(a)

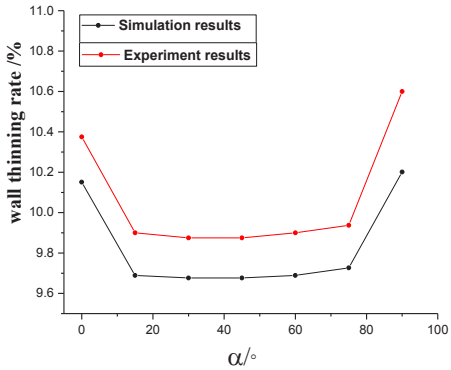

(b)

Fig.3. Wall thickening/thinning rate distribution of bent tubes: (a) wall thickening rate at the extrados; (b) wall thinning rate at the intrados.

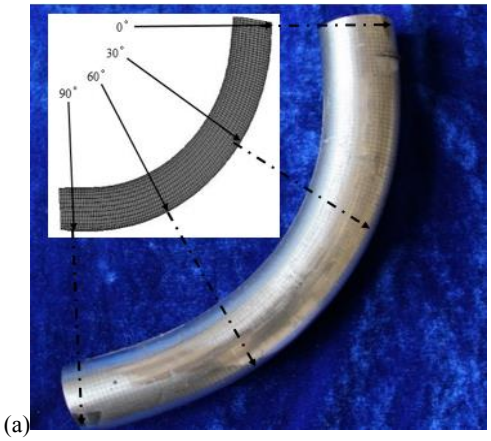

(a)

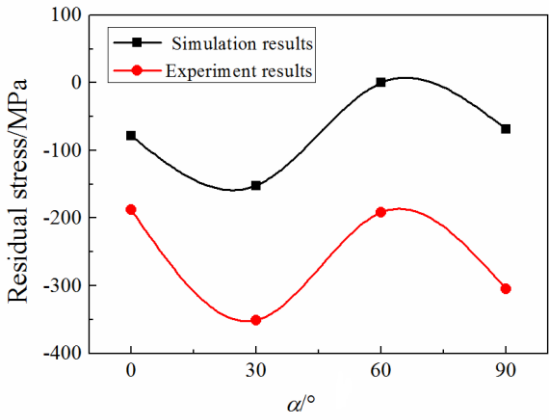

(b)

Fig.4. The residual stress distribution of the bent tube: (a) Point position; (b) The residual stress.

3 Result and Discussion

During the bending process, the tube and the die are in contact and have a relative motion which produces deformation in tube. The exterior wall thickness decreases due to the tensile stress, while the interior wall thickness increases due to the compressive stress. The FE model is used to study the contact behaviour during the process, and the wall thickness along with the change of the coefficient of friction, relative bending radius and the bending speed.

3.1 Contact behaviour during the push bending

Fig.5 shows the contact status during push-bending. It is found that the tube was not always in contact with the inner wall of the die closely. The yellow region in the figure means in which place the tube and the die was in contact. Along with the bending process, more and more sections had a deformation and this cause gaps between the die and the tube. As shown in Fig. 5(b) (c), an arc area appeared in which the tube and the die were in contact. At the meantime, a characteristic region at the top and the bottom of the tube was always in contact with the die until the unloading process.

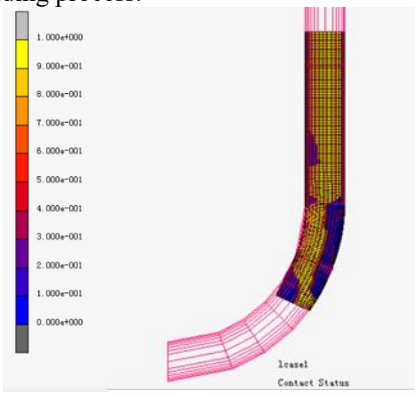

(a)Step 200

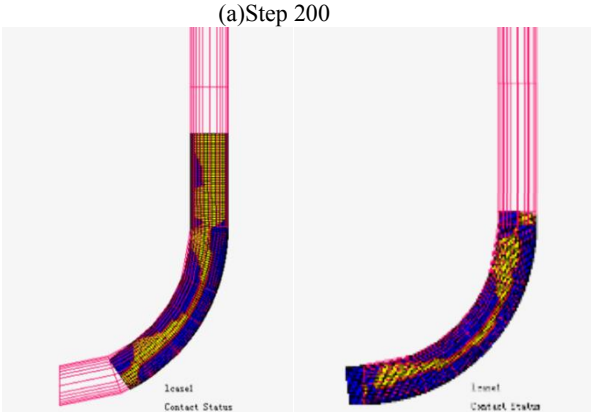

(b) Step 350 (c) Step 500

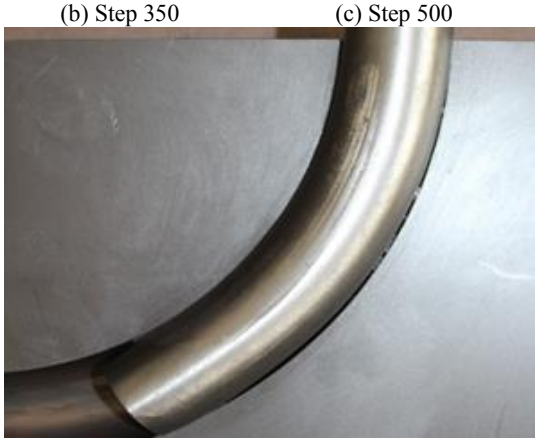

(d) Push-bending experiment

Fig.5. Contact status of different time steps :(a) Step 200; (b) Step 350; (c) Step 500.

3.2 The effects of friction coefficient

In the push-bending process, the exterior wall thickness decreases, and the interior wall thickness increases. Usually, the wall thinning rate and the wall thickening rate, as shown in Eq. (1) and Eq. (2), are used to express the two different wall thickness changes above.

Wall thinning rate at the extrados:

$$I_{ti} = t_{min}/t*100\% \quad (1)$$

Wall thickening rate at the intrados:

$$I_{ta} = t_{max}/t*100\% \quad (2)$$

Where t is the original wall thickness of the tube. t_{min} is the wall thinning at the extrados. t_{max} is the wall thickening at the intrados.

Fig.6 (a) (b) show the effects of friction coefficient on the wall thickness at the extrados and intrados separately. With the increase of friction coefficient, the wall thinning rate decreased at the extrados, and the thickening rate increased at the intrados. During bending, the metal flow occurs at the exterior wall because of the axial tension stress. The increase of friction coefficient can hinder the metal flow and reduce the thinning rate. At the meanwhile, the increasing friction coefficient hinders the metal flow at the interior wall, intensifying the wall thickening rate.

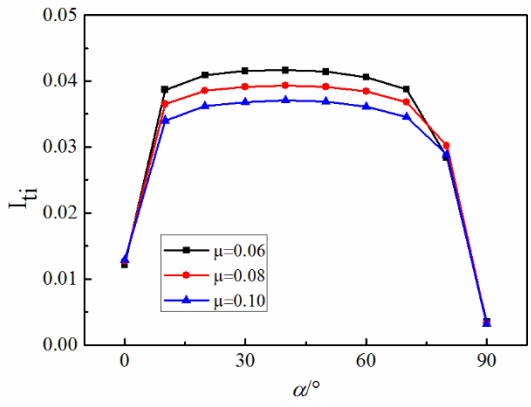

(a) Thinning rate

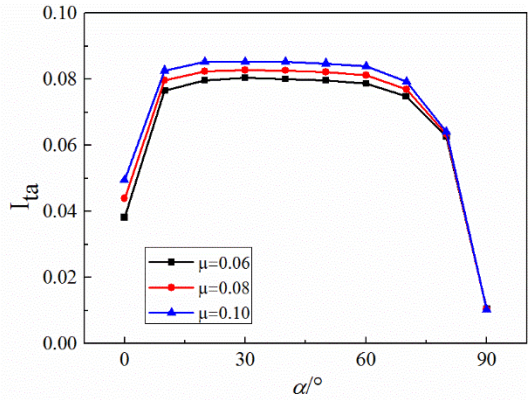

(b) Thickening rate

Fig.6. Effects of friction coefficient on thickness of tube

3.3 The effects of relative bending radius

Fig.7 (a) (b) show the effects of relative bending radius on the wall thickness. When the relative bending radius R/D is 3, 3.5, 4, the maximum value of the thinning rate was 4.64%, 4.37, 4.12%, and the maximum thickening rate was 10.79%, 9.17, and 8.04%. Along with the increases of the relative bending radius, both the wall thinning rate and the wall thickening rate decreased. When the relative bending radius is too small, it will be hardly to get a bent tube with high quality. Also, the wall thickening rate was significantly higher than the thinning rate. The tube is more likely to wrinkle than to rupture.

3.4 The effects of pushing speed

Fig.8 shows the thinning rate and the thickening rate with the increase of the pushing speed. The maximum value of the thinning rate was 4.19%, 4.17%, 4.16, and the maximum value of the thickening rate was 8.01%, 8.03%, 8.04%. Both the interior wall and the exterior wall changed a little. When the pushing speed increased from 6mm/s to 10mm/s, the thinning rate decreased by 0.03%, and the thickening rate increased by 0.03%. The effects of the pushing speed were very little.

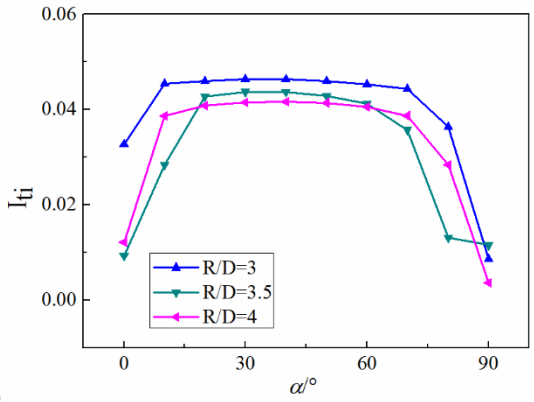

(a)

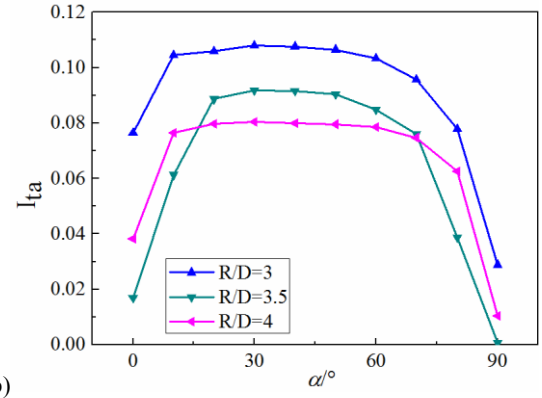

(b)

Fig.7. Effects of relative bending radius on thickness of tube: (a) thinning rate; (b) thickening rate.

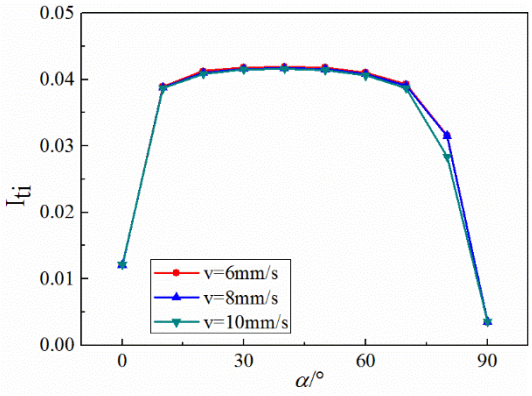

(a)

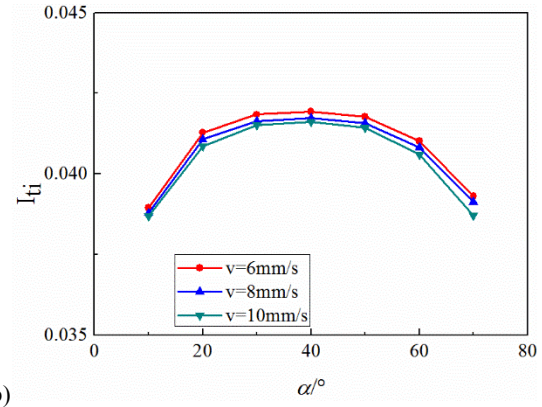

(b)

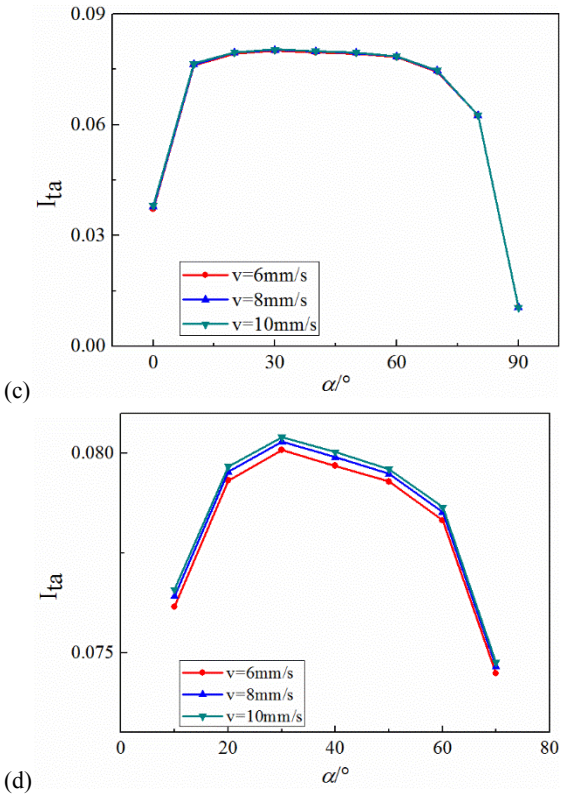

Fig.8. Effects of pushing speed on the wall thickness: (a) thinning rate; (b) thinning rate in the middle; (c) thickening rate; (d) thickening rate in the middle.

5 Conclusion

The FE model was established of push-bending to study the deformation behaviour, and results were compared with the experimental results. The contact status of different steps showed where the tube and the dies are in contact closely and where are not. For the push-bending, the wall thickness changes with the technological parameters. With the increase of friction coefficient or bending speed, the thinning rate decreased and the thickening rate increase. When bending speed changed from 6mm/s to 10mm/s, the wall thickness changed only a little. Both the thinning rate and thickening rate increased when a smaller relative bending radius was used. As a result, to push-bend a large radius tubes, a good lubricating condition which will help to ensure a better forming quality.

This work was supported by the International Science & Technology Cooperation Program of China [No. 2015DFR60370] and the Fundamental Research Funds for the Central Universities [No.DUT17GF209].

References

1. Wen T. On a new concept of rotary draw bend-die adaptable for bending tubes with multiple outer diameters under non-mandrel condition. J MATER PROCESS TECH. **214(2)**,311-317(2004)
2. Yang H, Lin Y. Wrinkling analysis for forming limit of tube bending processes. J MATER PROCESS TECH. **152(3)**,363-369(2004)
3. Li H, Yang H, Zhan M, Gu RJ. The interactive effects of wrinkling and other defects in thin-walled tube NC bending process. J MATER PROCESS TECH. **s187-188(3)**,502-507(2007)
4. Li H, Yang H, Zhan M, Kou YL. Deformation behaviours of thin-walled tube in rotary draw bending under push assistant loading conditions. J MATER PROCESS TECH.**210(1)**,143-158(2010)
5. El Megharbel A, El Nasser GA, El Domiaty A. Bending of tube and section made of strain-hardening materials. J MATER PROCESS TECH. **203(1-3)**,372-380(2008)
6. Al-Qureshi HA. Elastic-plastic analysis of tube bending. International Journal of Machine Tools and Manufacture. **39(1)**,87-104(1999)
7. Al-Qureshi HA, Russo A. Spring-back and residual stresses in bending of thin-walled aluminium tubes. MATER DESIGN. **23(2)**,217-222(2002)
8. Zhan M, Yang H, Huang L, Gu R. Springback analysis of numerical control bending of thin-walled tube using numerical-analytic method. J MATER PROCESS TECH. **177(1-3)**, 197-201(2006)
9. Daxin E YL. Springback and time-dependent springback of 1Cr18Ni9Ti stainless steel tubes under bending. Materials and Design.**31(3)**, 1256-1261（2010）
10. Lim H, Lee MG, Sung JH, Kim JH, Wagoner RH. Time-dependent spring back of advanced high strength steels. INT J PLASTICITY. **29(1)**, 42-59(2012)
11. Jiang ZQ, Yang H, Zhan M, Xu XD, Li GJ. Coupling effects of material properties and the bending angle on the spring back angle of a titanium alloy tube during numerically controlled bending. MATER DESIGN. **31(4)**, 2001-2010(2010)